RSC Advances

ROYAL SOCIETY OF CHEMISTRY

www.rsc.org/advances

Graphical Abstract

1D-2D SiC_{NWs}-GNPs hybrid nanofillers could make epoxy composites not only excellent thermal conductivity but also retain high electrical insulation.

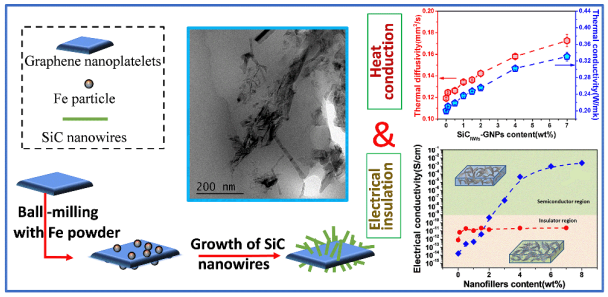

Journal Name

RSCPublishing

ARTICLE

Epoxy Composites Filled with One-dimensional SiC nanowires—two-dimensional Graphene Nanoplatelets Hybrid Nanofillers

Cite this: DOI: 10.1039/x0xx00000x

Received ooth xxxx 201x
Accepted ooth xxxx 201x

DOI: 10.1039/x0xx00000x

www.rsc.org/

Yi Wang,[a] Jinhong Yu,*[a] Wen Dai,[a] Dong Wang,[a] Yingze Song,[a] Hua Bai,[a] Xufeng Zhou,[a] Chaoyang Li,[b] Cheng-Te Lin,*[a] Nan Jiang*[a]

In this work, epoxy composites reinforced by one-dimensional (1D) SiC nanowires (SiC_{NWs})-two-dimensional (2D) graphene nanoplatelets (GNPs) hybrids have been prepared using a simple curing process. The direct iron-catalyzed heat-treatment process was designed to grow SiC nanowires on the surface of graphene nanoplatelets, acquiring a particular 1D-2D nanostructure. The SiC_{NWs}-GNPs hybrid nanofillers were characterized by scanning electron microscopy, X-ray diffraction, energy-dispersive X-ray spectroscopy, transmission electron microscopy, high resolution transmission electron microscopy, selected area electron diffraction, FT-IR spectrum and Raman spectroscopy. These analyses confirmed that single-crystalline β-SiC nanowires had been successfully fabricated with the solid carbon source (GNPs). In addition, the thermal and electrical properties of the epoxy composites with 1D-2D hybrid nanofillers fillers were investigated. The bridging effect of SiC nanowires contributed to the homogeneous dispersion of nanofillers in the polymer matrix, which is the key factor for enhancement of the properties of composites. In particular, the thermal conductivity of epoxy composite with 7 wt% SiC_{NWs}-GNPs is 65.2% higher than that of neat epoxy, while the electrically insulating properties of the composite is still reserved.

1. Introduction

Graphene nanoplatelets (GNPs) with a two-dimensional (2D) platelet structure are consisted of a few stacked graphene platelets which correspond to partially exfoliated graphite liked graphite nanocrystals with multi-graphene layers. Due to extraordinary mechanical[1], electrical[2] and thermal[3] properties of GNPs, an extensive amount of interest has been casted to the polymer composites filled with carbon-based nanofillers. The remarkable performance is ascribed to large specific surface area of graphene and its exceptional properties such as high in-plane electrical mobility, thermal conductivity and Young's modulus.[4] In the past decade, graphene sheets have been incorporated into a wide range of polymer matrix, including epoxy,[5] polyimide,[6] nylon-6[7] etc., for multiple applications. However, in many situations, the potential applications of GNPs are limited because GNPs are likely to restack and agglomerate due to large Van der Waals forces and strong π-π interactions between GNPs planar nanosheets.[8, 9] To ensure effective reinforcements in the polymer composites, the good dispersion and strong interfacial bonding between the GNPs and the polymer matrix have to be guaranteed.[10] The typical strategy employed for the preparation of well dispersed graphene-based nanocomposites is to utilize many different surface treatment and functionalization techniques for the graphene oxide (GO). To date, the mixing of graphene and functionalized graphene with polymers covers the most of the published studies[4, 11]. For example, polydopamine (PDA), a synthetic polymer that mimics mussel adhesive proteins (MAPs), has been used as a functional coating on clay[12] and graphene[13]. However, it should be pointed out that the covalent attachment of graphene to polymer chains can improve some properties, but may be negative for others, especially those related to the movement of electrons or phonons.[14] Meanwhile, the preparation process of composites would contain lots of procedures and often require large amounts of organic solvents.[15] Hybrid nanomaterials, composed of two or more different fillers can be designed to achieve a synergistic effect and endow a polymer matrix with better performance.[16] In addition, when it comes to hybrid nanofillers, it can be expected that

[a]*Key Laboratory of Marine New Materials and Related Technology, Zhejiang Key Laboratory of Marine Materials and Protection Technology, Ningbo Institute of Material Technology and Engineering, Chinese Academy of Sciences, Ningbo 315201, China. E-mail address: **yujinhong@nimte.ac.cn,linzhengde@nimte.ac.cn,jiangnan@nimte.ac.cn***

[b]*Research Institute& School of Systems Engineering, Kochi University of Technology, Kami city, Kochi 782-8502, Japan.*

the agglomeration of the nanoparticles and interfacial interaction problems in polymer composites could be solved simultaneously by using such functional hybrid nanofillers.[17] For instance, Luan et al. [18] reported that epoxy composites containing 1-D Ag nanowires and 2-D chemically reduced graphene hybrid fillers demonstrate synergetic effects and the hybrid fillers also act as combined physical and chemical crosslinking site for polymer matrix. Similarly, a strategy was designed to incorporate carbon nanotube and graphite nanoplatelet into the epoxy resin. It is the long and tortuous carbon nanotube that can bridge adjacent graphite nanoplatelet and restraint their aggregation, resulting in the thermal conductivity enhancement of epoxy composites.[19] Another hybrid composite material was developed by Palza and co-workers[20] preparing poly(propylene) (PP)/CNT materials with clay particles. The presence of well-dispersed clay particles drastically decreases the electrical conductivity of the resulting material. The hybridization of 1D nanofillers and 2D lamellar flakes thus leading to 3D network structure is crucial, as it can enable outstanding performances and tailor-made properties compared with individual nanomaterials.

In the present study, we demonstrate the use of reduced iron powders as a catalyst for the growth of SiC nanowires (SiC_{NWs}) on the GNPs followed by incorporation of the as-prepared SiC_{NWs}-GNPs hybrid nanofillers into epoxy (EP) matrix to make epoxy composites. To our best of knowledge, it is the first time to synthetize SiC_{NWs} on the GNPs with a simple heat-treatment process. Our results show that we attach the surface of GNPs with a SiC nanowires in order to prepare a thermally conductive, but electrically insulating, GNPs-based hybrid nanofillers. Sequentially, we investigated the effect of hybrid nanofillers on thermal and electrical properties of epoxy composites.

2. Experimental

2.1. Materials

Commercial graphene nanoplatelets (GNPs) were produced by Ningbo Institute of Materials Technology and Engineering, Chinese Academy of Sciences (China). The silicon powder with average size of 1 μm and a purity of > 99.9% was supplied by Shanghai ST-Nano Science&Technology Co., LTD (China). The iron powder reduced was purchased from Sinopharm Chemical Reagent Co., Ltd. (China). Epoxy resin (E51, Shanghai Polyrich Int'l Trading Co., Ltd., China) along with hardener of diethylenetriamine (DETA, Sinopharm Chemical Reagent Co., Ltd., China) was used in the present study. All other chemicals were analytical reagent grade and used without further purification.

2.2. Preparation of SiC_{NWs}-GNPs Hybrids

The growth of SiC nanowires on the graphene nanoplatelets surface was carried out by a simple heat-treatment process, in which the mixture of GNPs (black), silicon powders, Fe addition were used as the source materials. In the typical experiments, 0.2 g GNPs, 0.4 g silicon powders and 0.6 g reduced Fe powders were began with a ball-milling process for 12 hours. The as-milled powders were first set in a graphite crucible and then placed in the vacuum induction furnace that was pumped to abase pressure of about 10^{-3} Pa. Afterwards, the furnace was heated from room temperature to 1300 °C and maintained for reaction for 90 min under a total pressure of about 10^{-5} Torr. After the growth process the furnace was switched off and the sample cooled down at room temperature. For purification of nanomaterials, the extra silicon powders and Fe particles were simply sieved out by dispersing in the deionized water with ultrasonically vibration, the resulting gray nanofillers were dried overnight in vacuum for 80 °C.

2.3. Preparation of SiC_{NWs}-GNPs/epoxy composites

Epoxy composites containing different SiC_{NWs}-GNPs contents (from 0 to 7 wt %) were prepared by the following procedures. A desired amount (0, 0.1, 0.5, 1.0, 1.5, 2.0, 4.0 and 7.0 wt %) of nanofillers were dispersed in acetone in an ultrasonic bath for 0.5 h and then added into the epoxy with 0.5 h of ultrasonication. The homogeneous mixture was put in a vacuum oven at 60 °C overnight to remove the solvent. DETA (weight ratio of epoxy: DETA=3: 0.338) was added to the mixture, which was then mixed with a Flacktek Speedmixer at a speed of 3000 rpm for 5 min before being transferred to a PTFE mold. The curing conditions were 12 h at room temperature and then 1h at 80 °C. Its synthetic route and the preparation sketch of composites are shown in **Scheme 1**.

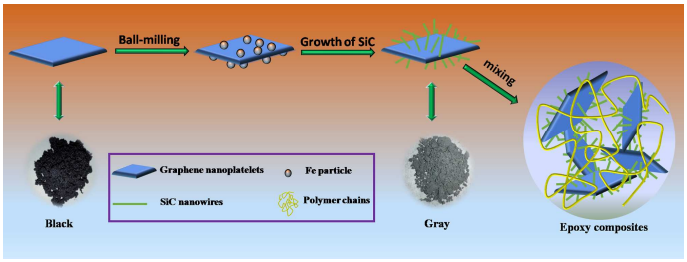

Scheme 1 Synthetic process for the epoxy composites.

2.4. Characterization

The X-ray diffraction (XRD) patterns of the samples were recorded on a D8 DISCOVER With GADDS (BRUKER Ltd. Germany) with CuKα radiation (λ=1.5406Å). The scanning was performed from 10° to 80° with a speed of 4 °min^{-1} at room temperature. The Raman spectra was recorded using a Reflex Raman System (RENISHAW plc, Wotton-under-Edge, UK) employing a laser wavelength of 532 nm. Fourier transform infrared (FTIR) spectra were carried out using a Nicolet 6700 FTIR (Thermal scientific Inc. USA) between 400 and 4000 cm^{-1}. Dried filler was mixed with KBr powders and pressed into tablets for characterization. The microstructures of obtained samples and the composites were obtained from JEOL JEM-2100 (Japan Electron Optics Laboratory CO., Ltd, Japan) instrument with an acceleration voltage of 200 KV. The prepared powers were dispersed in ethanol by sonication for 15 min and some pieces were collected on 200 mesh carbon coated copper grids. For the epoxy composites, the approximate 70 nm nanoplatelets samples were prepared using an ultra microtome (LKB Nova) equipped with a diamond knife and subsequently placed on copper grids for TEM observations. The fracture surface of the composites was examined on field emission scanning electron microscopy (FE-SEM, QUANTA FEG250, USA) at an acceleration voltage of 20 kV. Samples were broken and the fractured surface was coated with a thin layer of gold powder to avoid the accumulation of charge and improve conductivity. Thermogravimetric analysis (TGA) was carried out with a Perkin-Elmer Pyris Diamond TG/DTA thermo-

analyzer. The temperature ramp rate was 10 °C/min in nitrogen or air atmosphere. Thermal conductivities of the composites were measured with LFA 457 Nanoflash apparatus (NETZSCH, Germany) at room temperature. The samples were prepared in square-shaped forms, with length of 10 mm and a thickness about 1.2 mm. The thermal diffusivity values (mm^2/s) of the composites were recorded. Dynamic mechanical analysis (DMA) performed on a DMA Q800 dynamic mechanical analyzer (TA Instruments, USA) to determine modulus and glass transition temperature (Tg). The tests were carried out in the single cantilever mode from 50 to 250 °C at a heating rate of 1 °C/min. The electrical conductivity and permittivity of neat epoxy and epoxy composites were measured by broad frequency dielectric spectrometer (Novocontrol Concept 80) with the frequency range from 1 to 10^6 Hz. Composite samples were placed between two gold-plated brass electrodes that were pressed together with a micrometer screw.

3. Results and discussion

3.1. Characterization of SiC_{NWs}-GNPs nanofillers

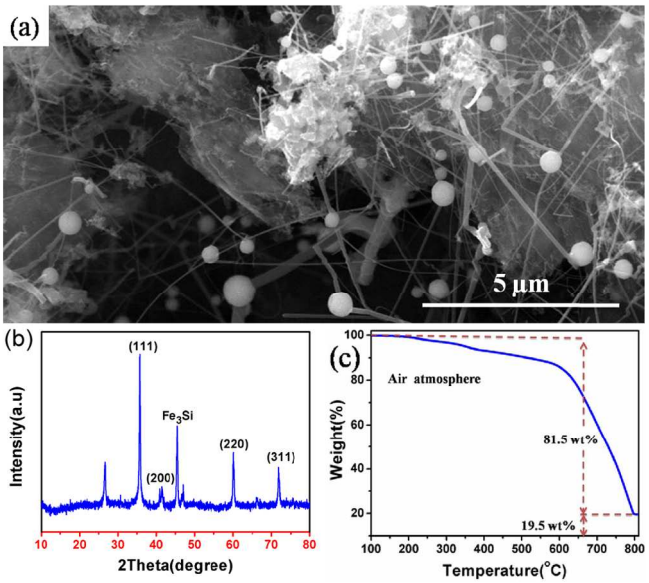

Fig.1. (a) SEM image, (b) XRD pattern and (c) TGA curve of the SiC_{NWs}-GNPs nanofillers.

The typical SEM image of the SiC_{NWs}-GNPs nanofillers is shown in **Fig.1a**. It can be found that large quantities of randomly oriented wire-like products have been synthesized on the surface of GNPs. The diameters of the nanowires range from 50 to 100 nm and the length is generally several micrometers. The X-ray diffraction (XRD) measurements are conducted on the prepared product to assess the overall structure. **Fig.1b** displays XRD pattern of as-received fillers. In the pattern, four diffraction peaks can be indexed as (111), (200), (220), and (311) reflections of face-centered cubic cell of β-SiC, which has the lattice constant of a= 4.348 Å. These values agree well with the standard values for β-SiC (JCPDS card No. 73-1708). Moreover, the two weak diffraction peaks (centered at 26.6°, 47.1°) corresponding to the GNPs are also found. The XRD result also indicates the existence of Fe_3Si in the products, which is consistent with the Fe-C-Si alloy in Fe-catalyzed SiC nanowires vapor–liquid–solid (VLS) growth process (**Figure. S1**). **Fig.1c** show the TGA plot of as prepared SiC_{NWs}-GNPs nanofillers in the air atmosphere. It can be seen from the picture that the weight yield at 800 °C is about 19.5%. A main weight loss steps at around 200-800 °C was from the thermal decomposition of the GNPs structure. The SiC_{NWs}-GNPs nanofillers show a fast thermal degradation with 81.5 wt% loss during the thermo-gravimetric process in the air atmosphere. Meanwhile, the residual inorganic phase (mostly SiC) accounts for a small portion.

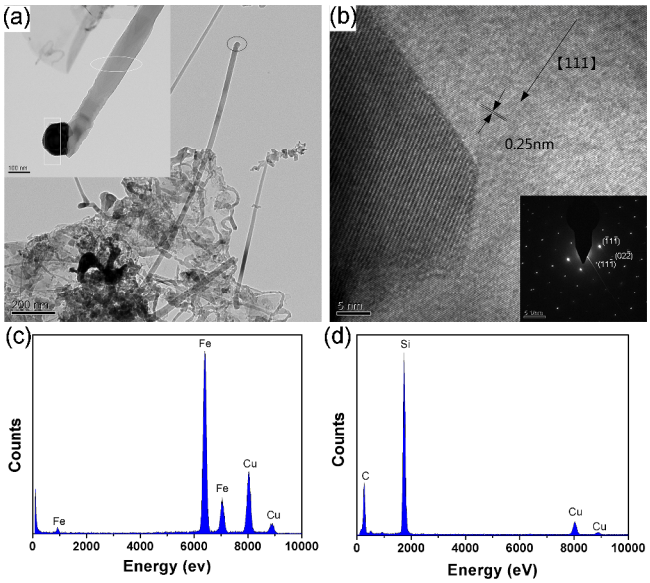

Fig.2 (a) TEM image (Left top inset: the local magnified image of nanowires) of obtained sample (b) Typical HR-TEM image of the 1D nanostructures and its representative corresponding selected-area electron diffraction (SAED) pattern. The related EDX spectrums taken from the different positions of nanowires (c) on the tip (d) on the middle position.

In order to characterize the detailed structure of the SiC_{NWs}-GNPs nanofillers, TEM image and HR-TEM image corresponding SAED patterns are shown in **Fig. 2a** and **Fig. 2b**. **Fig. 2a** shows the nanowires with smooth surfaces and very inhomogeneous diameters were obtained under the Fe-catalyst condition. At the same time, we can observe that the nanowires are mainly straight and discretionarily grown on the surfaces of GNPs. The local magnified image of nanowires (Left top inset in **Fig. 2a**) obviously shows a characteristic TEM image of the spheres at the tips of nanowire, which further suggests that the resulting nanowires are grown by the VLS mechanism.[21, 22] Also, **Fig. 2b** shows that the HR-TEM image that the distance between two adjacent lattice planes perpendicular to the growth direction of the wire (marked with black arrow) is about 0.25 nm, which is consistent with the spacing of (111) plane of β-SiC (JCPDS card No. 73-1708). Therefore, combined with the XRD analysis of the products, it can be safely concluded that the nanowire stem is single-crystalline SiC and the growth direction is [111]. Their corresponding SAED pattern is shown in the inset of **Fig. 2b**, the spot patterns $(\bar{1}1\bar{1})$, $(11\bar{1})$, $(02\bar{2})$ could be indexed to the cubic β-SiC structure and it matches well with [011] crystalline band diffraction. **Fig. 2c** and **Fig.2d** provide two related EDX spectrums taken on the different positions of the nanowires. The spherical cap (marked with white square in **Fig. 2a**) containing iron is observed only on the tip of the nanowires. In addition, only the Si and C are detected by EDX analysis of the middle part of the nanowire (corresponding to white circle in **Fig. 2a**), indicating a pure Si-C chemistry in nanowires. The Cu signals come from copper grid of

the TEM sample holder. It demonstrated that the achieved nanostructures had a single-crystalline phase.

It is interesting to compare FTIR and Raman spectra as shown in **Fig. 3.** As can be seen from the FTIR spectrum, It shows two absorption bands from transversal optic (TO) mode Si-C vibrations (799 cm^{-1}), and longitudinal optic (LO) mode Si-C vibrations (972 cm^{-1}),which is in good agreement with previously reported value.[23] Meanwhile, in the Raman spectrum, a sharp strong peak centered at 785 cm^{-1} is originated from SiC TO mode and a small weak peak at 940 cm^{-1} is due to the SiC LO mode. This results show corresponding number red shift of 11 and 32 cm^{-1} respectively compared with the modes of bulk SiC.[24] The reason for this exception may originate from the confinement effect, stacking faults and inner stress from the twin crystal structure of SiC nanowires.[25] At the same time, the presence of carbon is readily detected because of its large Raman cross section. These three carbon-related peaks correspond to the D-band, G-band and 2D-band of GNPs, respectively. FTIR spectrum does not reveal remarkable carbon-related peaks, while the LO mode Si-C vibrations appeared obvious in FTIR is not clear in Raman spectrum. These results show the selective sensitivities of two spectrometers. Hence, together with the XRD, SEM, TEM, HRTEM and SAED analyses, it can be concluded that the single-crystalline β-SiC is successfully fabricated on the surface of GNPs, forming a unique structure in which a 2D GNPs has several 1D SiC nanowires attached to it.

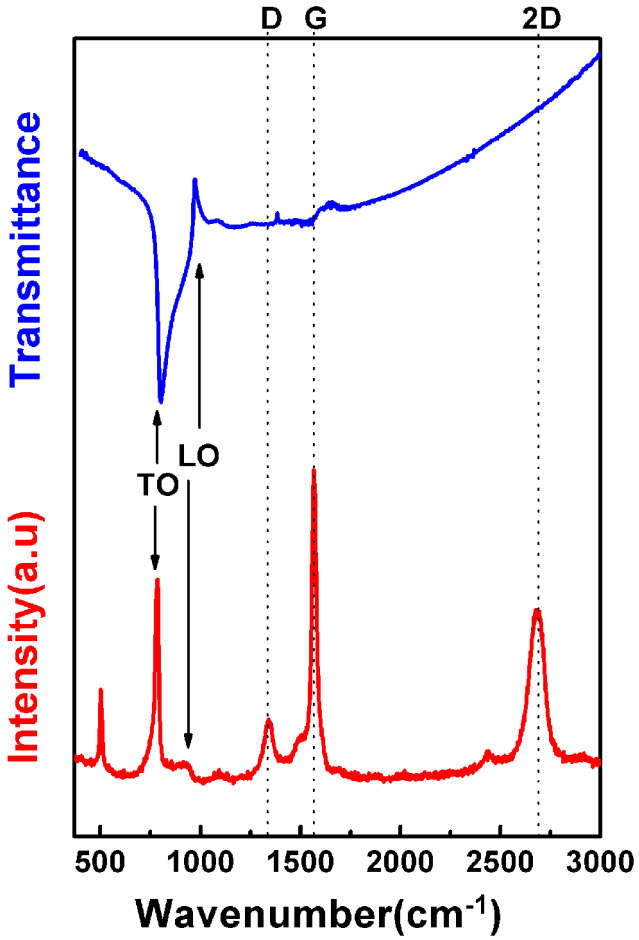

Fig. 3. Comparison of FTIR and Raman spectra of SiC_{NWs}-GNPs nanofillers.

3.2. Structural characterization of composites

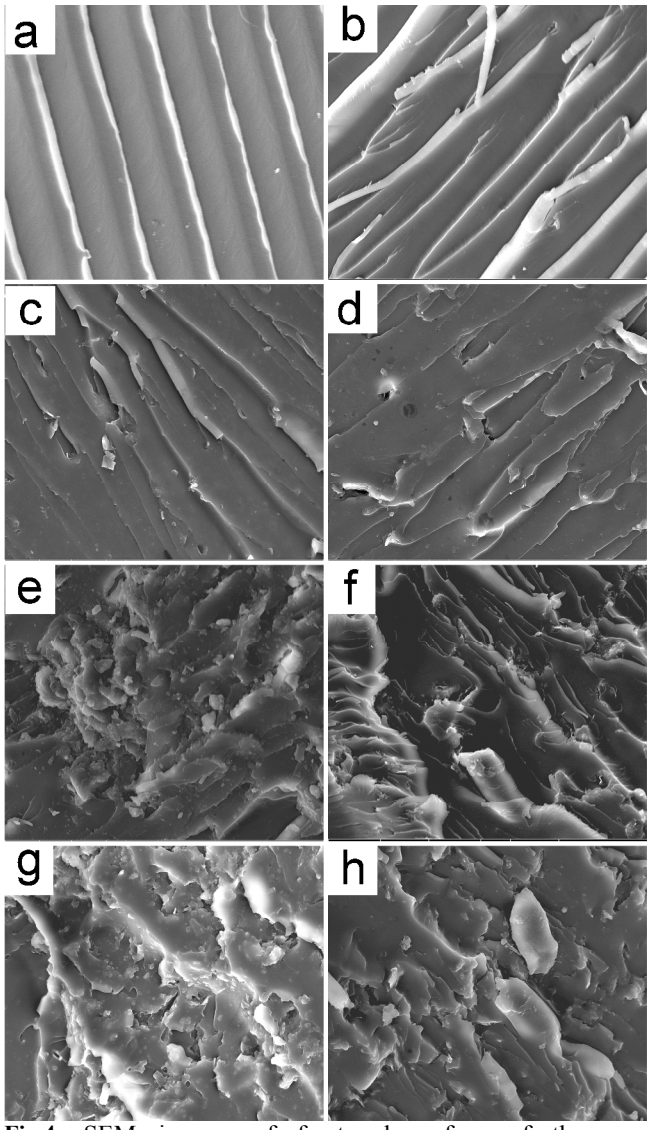

Fig.4. SEM images of fractured surface of the epoxy composites containing different 1D-2D SiC_{NWs}-GNPs nanofillers loadings: a)0wt%, b)0.1wt%, c)0.5wt%, d)1.0wt%, e)1.5wt%, f)2.0wt%, g)4.0wt% and h)7.0wt%.

In order to understand the relationship between structure and properties of neat epoxy and epoxy composites, the fracture surfaces of the samples are characterized with SEM, as shown in **Fig. 4**. For the neat epoxy resin in **Fig. 4(a)**, it could be obviously seen that neat epoxy exhibited a relatively smooth and typical stripe structures with cracks almost parallel to the crack propagation direction, which is typical of a brittle thermosetting polymer. The fracture surfaces of composites (**Fig. 4(b-d)**) are similar to the neat epoxy and reveal a rougher and more irregular feature, indicating the characteristic of toughening factor. With the increasing incorporation of the hybrid nanofillers, the fracture surfaces of the epoxy composites presented considerably different fracture graphic features, as shown in **Fig. 4(e–f)**. It can clearly be seen that a rougher fracture surface, and numerous tortuous and indentations and deep cracks can be observed. The fracture stripes transform from mainly parallel orientations to totally different directions, suggesting a strong filler-polymer interfacial adhesion, thus forming efficient stress transfer

from the matrix to the fillers. Meanwhile, no apparent aggregated effects occur at high SiC_{NWs}-GNPs loading levels (See **Figure. S2**), it is believed that the SiC nanowires grown on the GNPs surface could inhibit the plane-to-plane aggregations of GNPs and the fillers/matrix interfacial properties could be also improved.

3.3. Thermal properties of composites

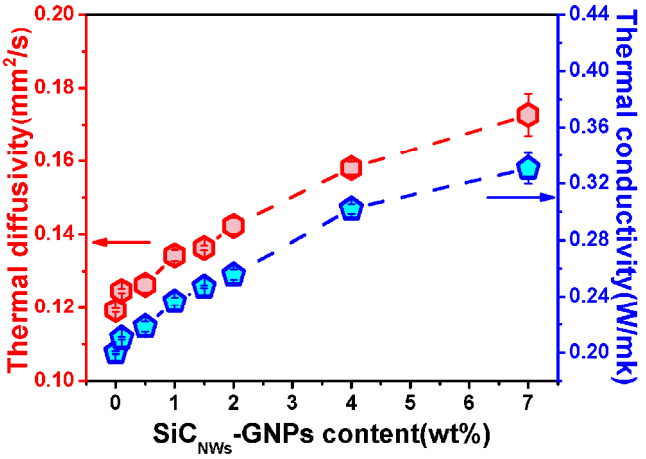

Fig.5. Thermal diffusivity and thermal conductivity of epoxy composites.

The thermal conductivity and diffusivity of epoxy composites containing 1D-2D hybrids SiC_{NWs}-GNPs nanofillers were examined as a function of the fillers content and the results are shown in **Fig.5.** It is evident that the thermal conductivity increases steadily with the incorporation of the SiC_{NWs}-GNPs nanofillers. In addition, the thermal diffusivity of the composites shows almost the similar trend. The thermal conductivity of pure resin is approximately 0.20 W/m·K. At 7 wt% of nanofillers loading, an increment by 65.2% is observed as compared to neat epoxy. This increasing tendency promises higher thermal conductivity at a larger SiC_{NWs}-GNPs content. It is well-known that thermal conductivity is affected by the carbon nanofiller structure quality within the matrix, loading, dispersion, and thermal resistance of the interface between nanofillers and the polymer matrix.[26-28] The thermal conductivity of epoxy composites at low filler levels (up to 2% loading) merely show a merely a little improvement of thermal conductivity value. This is because the fillers in polymer matrix are in an isolated state which is similar to the "sea-island" structure, thus, the number of nanofillers in the epoxy resin would be not enough to form a continuous network. By contrast, when the hybrid fillers contents go up to a higher level (4-7 wt%), the thermal conductivity increases at a higher speed. This phenomenon may be attributed to several factors.[29] Firstly, the contact geometry changes from the 0-D point contact to 1-D linear contact, increasing the contact area within the hybrid nanofillers considerably. Secondly, the SiC nanowires grown on the surface of GNPs can bridge adjacent nanofillers and inhibit aggregation of GNPs, containing intrinsic high surface of GNPs to contact with polymer matrix. While it is noted that the interface between the SiC nanowires and GNPs might act as phonon scattering sites[30] for phonon transport because of the acoustic impedance mismatch at the interface.[31] In short, the improvement of the thermal conductivity is on the account of the integrated factors mentioned above.

Thermal stability is one important property for epoxy based composites used as high-performance engineering plastics. TGA/DTG profiles for neat epoxy and its composites as a function of temperature at the heating rate of 10 °C/min are shown in **Fig. 6.**

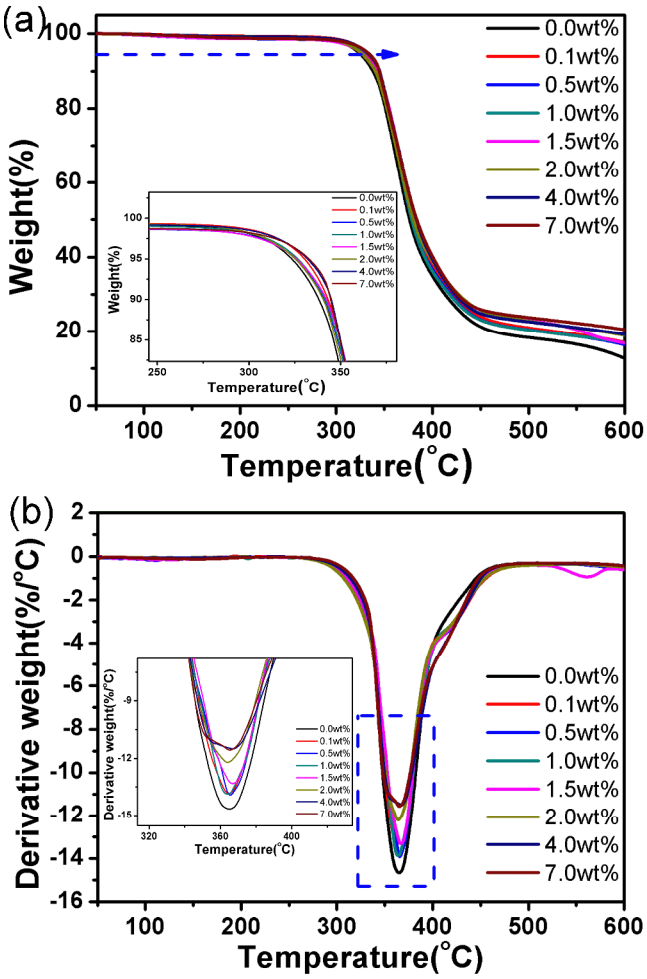

Fig.6. (a) TGA and (b) DTG curves of the neat epoxy and its composites.

It is apparently seen that all the samples exhibit similar thermal behaviour and only one-step decomposition, suggesting that the existence of nanofillers did not significantly alter the degradation mechanism of the epoxy matrix. As shown in **Fig. 6a**, the main weight loss takes place at around 350-450 °C, which is attributed to the degradation of epoxy network.[32] The characteristic thermal parameters selected were the temperature for 5% weight loss ($T_{d5\%}$) and maximum degradation temperature, which is the highest thermal degradation rate temperature. As can be seen from **Table 1**, it is observed that the $T_{d5\%}$ of the neat epoxy resin is 323.3°C. While the $T_{d5\%}$ of epoxy composites with 0.1, 0.5, 1.0, 1.5, 2.0, 4.0 and 7.0 wt% SiC_{NWs}-GNPs hybrid nanofillers are 330.3, 325.5, 326.5, 325.7, 325.2, 331.7 and 332.6 °C. **Fig.6a** reveals that all epoxy composites show increase in $T_{d5\%}$ in comparison with these of the neat epoxy. It is also noted the char yields of all composites are increased as compared to neat epoxy. Moreover, as can be seen from the DTG curves, the maximum degradation temperature (T_{max}) of the materials is also slightly improved by addition of the nanofillers. It is believed that the formation of compact chars of hybrid nanofillers and polymer matrix during the thermal degradation is beneficial to the improvement of thermal stability of the composites.[33] At the same time, 1D-2D nanostructures of the nanofillers increase the crosslinking sites between the fillers and matrix, thus restricting thermal motion of the polymer chains and the mobility of the polymer segments at the interfaces of epoxy.[34]

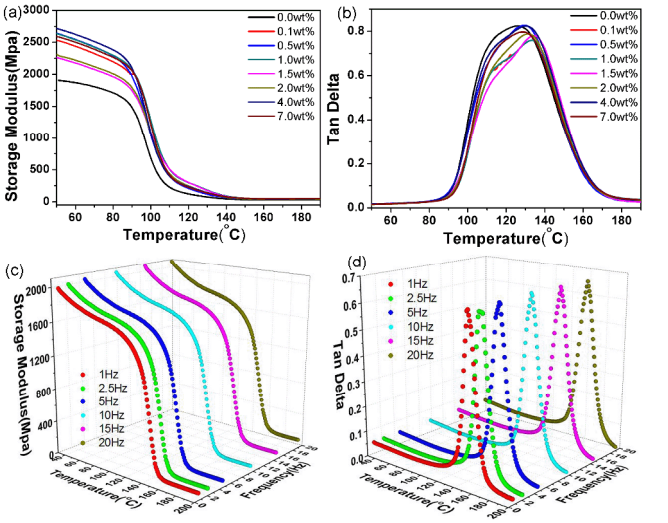

Fig.7. Dynamic mechanical analysis of neat epoxy and its composites: (a) storage modulus (E') and (b) tanδ. (c)Storage modulus spectra (d) loss factor spectra as temperature and frequency for epoxy composites containing 4 wt% SiC_{NWs}-GNPs nanofillers loadings.

To gain further insight into the interfacial interactions, the epoxy contained nanoscale additives were characterized using DMA. **Fig.7** shows the variations in storage modulus and tan δ as a function of temperature from below the glassy state temperature range to the rubbery plateau of neat epoxy and its composites. The storage modulus represents the amount of energy that the polymer stores and is related to the stiffness and dampening capacity of material.[35] All the composite samples exhibit higher storage modulus (E') in the glass region than the neat epoxy, and the corresponding data are summarized in **Table 1**. In particular, the storage modulus of epoxy composite containing 4.0wt % SiC_{NWs}-GNPs hybrid nanofillers increases dramatically to 2719 MPa (at 50 °C) in the glassy region, which is 42.4% larger than that of neat epoxy (1910 MPa), indicating that the nanofillers are homogeneously dispersed and have strong interfacial adhesion with the matrix.[36] As the temperature increases, the storage modulus falls, indicating energy dissipation which occurs during the transition of the glassy state to a rubber state. It is obvious that the storage modulus of the composites appear much higher than that of the neat epoxy in the rubber state. For instance, the storage modulus at 120 °C was about 140 % higher than neat epoxy resin when filler content is 1.5 wt%. The loss factor tan δ defined as the ratio of the loss modulus to the storage modulus, which is very sensitive to a structural transformation in a solid material. The peak temperature of tan δ taken as the glass transition temperature (Tg). As can be seen from the **Fig.7b**, the Tg value of the composites all shifted to higher temperatures compared to neat epoxy. The detail data are also summarized in **Table 1**. These phenomena can be attributed to the facts that: (i) the presence of hybrid fillers in the composite will increase the hindrance of the segmental motion of the epoxy chains due to the effects of interfacial interactions and entanglements, (ii) the 1D-2D hybrid nanostructure and random orientation of SiC nanowires likely results in enhanced mechanical interlocking[1] with the polymer chains, (iii) To be more specific, the good miscibility between the 1D-2D hybrid nanofillers and epoxy matrix allows the nanosheets to be dispersed individually and homogeneously, which could maximize the filler's effect on reducing mobility of polymer chains. At the same time, we had investigated storage modulus spectra and loss factor spectra as temperature and frequency for epoxy composites containing 4 wt% SiC_{NWs}-GNPs nanofillers loadings, which is shown in **Fig.7c** and **Fig.7d**. It is obviously seen that storage modulus and loss factor have the similar trend at different frequency. With the increase of the test frequency, the value of storage modulus and glass transition temperature both shift to a higher area, which is consistent with the previous study.[37]

Table 1. TGA and DMA results of the epoxy composites

SiC_{NWs}-GNPs (wt%)	TGA data		DMA data	
	T_d[a]/°C	Char yield at 600°C (%)	Storage modulus[b]/Mpa	T_g/°C
0.0	323.3	12.7	1910	126
0.1	330.0	17.0	2535	133
0.5	325.5	16.4	2643	130
1.0	326.5	16.9	2635	133
1.5	325.7	16.8	2264	134
2.0	325.2	18.9	2315	131
4.0	331.7	19.2	2715	130
7.0	332.6	20.4	2593	129

[a]Temperature at 5% weight loss. [b]Storage modulus at 50 °C.

3.4. Electrical properties of composites

The AC electrical conductivity as a function of frequency for epoxy composites of different SiC_{NWs}-GNPs weight fractions is shown in **Fig. 8a**. All the samples show the typical insulating behaviour, consisting a continuous straight line at all frequencies.[38, 39] It should be noted that the addition of nanofillers into the epoxy matrix didn't display a dramatic increase of the electric conductivity, with merely two orders of magnitude improvement. The composites also didn't show an apparent transition behaviour from insulator to conductor, with a resistive behaviour at low frequencies and capacitive at high frequencies, as most carbon based composites did.[40] There can be frequency dependent response at higher frequencies for not fully percolated specimens, indicating that the addition of 7 wt% nanofillers still did not come to the percolation threshold. It is well-known that conductive fillers/insulating polymer composites becomes electrically conductive as the filler content exceeds a certain critical value attributed to a percolation phenomenon. The electrical conductivity increased slightly with the increasing SiC_{NWs}-GNPs content under saturation because of the bridging effect of SiC nanowires among the nanofillers, as indicated in the TEM image (**Figure. S3**). Modifying the GNPs sheets by synthetizing SiC nanowires on their surfaces dramatically affected the electrical conductivity. The semiconductor material, SiC nanowires, on the GNPs sheet can prevent electron tunnelling, thereby degrading the electrical properties of the composites.[31] This indicates that the SiC nanowires on the GNPs surface can prevent the direct contact between the GNPs and act as the role of bridge, thus hindering the formation of electrical pathways in the epoxy composites because the SiC nanowires disrupt conjugating electron transport and increase the tunnelling energy barrier. This can be further proved in **Fig. 8b**, it is observed that the addition of the hybrid nanofillers slightly increases the electrical conductivity of epoxy composites and the overall section in electrical conductivity belongs to insulator region. However, compared with our previous study (reference [10]), the epoxy composites filled with GNPs show a high efficiency to improve the electrical conductivity of material. The significant difference mentioned above could be interpreted by the probable models of nanofillers distribution in the matrix, as presented in **Fig. 8b**. Lower dielectric constant is one of the most wishful properties for next generation electronic devices. The novel nanostructure of the 1D-2D SiC_{NWs}-GNPs hybrid nanofillers inspired us to investigate

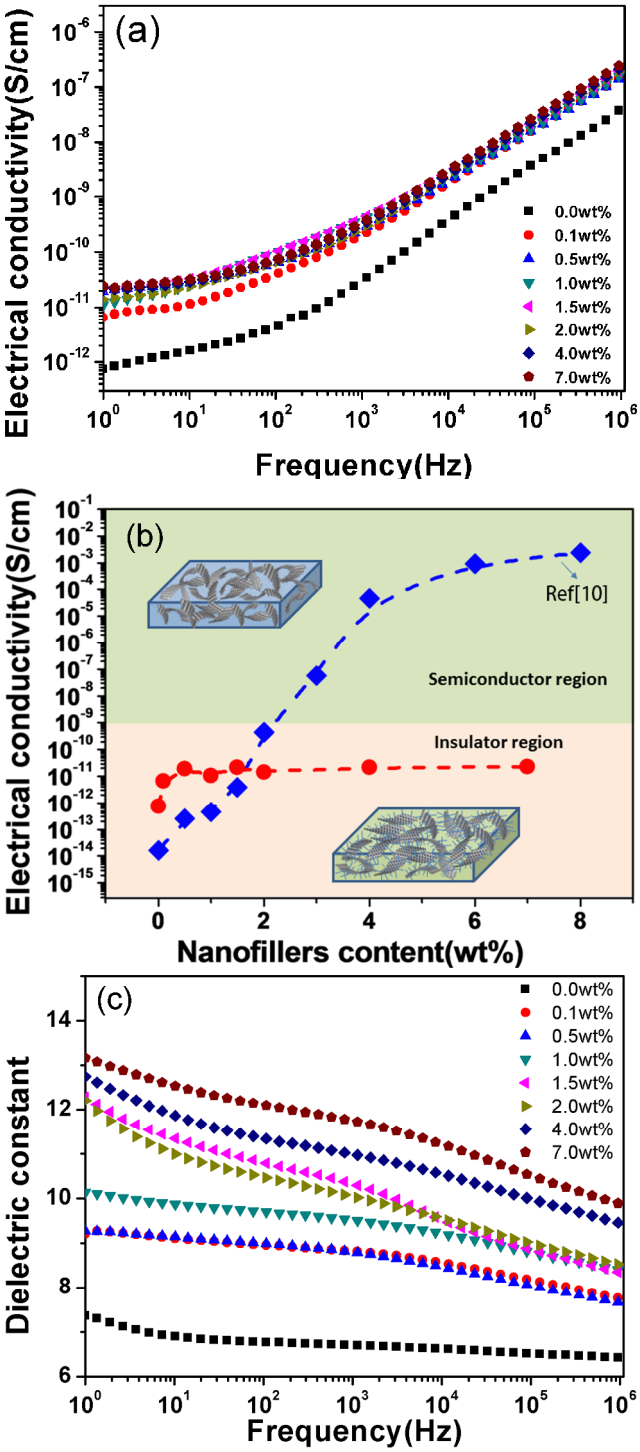

Fig.8 Dependence of (a) ac conductivity, (b) the dielectric constant of the epoxy composites on frequency at room temperature, (c) the electrical conductivity of composites with different SiC_{NWs}-GNPs concentrations at 1 Hz.

the dielectric properties. **Fig. 8c** gives the dielectric constant of epoxy composites with various nanofillers contents at room temperature. It can be seen that the dielectric constant of neat epoxy and epoxy composites decrease with increasing frequency, which can be explained by the fact that in the high frequency region dipole polarization in the epoxy functional groups and the interface dipoles cannot keep up with the variation of frequency under an applied electric field. The slight increase of dielectric constant can be mainly attributed to the interfacial polarization in heterogeneous epoxy system filled with nanofillers and to the mini-capacitor principle. With increase of nanofillers content in polymer phase, the isolation distances between adjacent nanofillers are continuously reduced. Nevertheless, when the nanofillers concentration comes to a certain degree, the SiC nanowires will restrict the final distance of the neighbouring nanofillers. Finally, a network of mini-capacitors with the SiC_{NWs}-GNPs as electrodes and a very thin epoxy layer in between as dielectric can be formed in the composite near percolation threshold. Each mini-capacitor contributes an abnormally large capacitance, which can then correlate with the corresponding increase in the dielectric permittivity.[41] This phenomenon was attributed to inhomogeneous composites were found to show better dielectric properties than the homogeneous composites.[42,43] This can further prove the 1D-2D hybrid nanostructure can effectively solve the disperation problem and obtain a homogeneous nanofillers reinforced composites.

4. Conclusions

In summary, SiC nanowires have been successfully grown via iron-catalyzed heat-treatment process on GNPs, forming 1D-2D hybrid nanofillers. With elementary purification, the as-prepared SiC_{NWs}-GNPs nanofillers were directly used to fabricate epoxy composites via simple curing procedure. It was employed to bridging effect of SiC nanowires attached to the GNPs so as to inhibit their aggregation and facilitate homogeneous dispersion within an epoxy matrix. As a result, the investigation on the thermal and electrical properties of the composites demonstrated that much improvement had been obtained with incorporating the hybrid nanofillers. Additionally, the epoxy composites with 7 wt% loading show 65.2% increment of thermal conductivity compared to that of neat epoxy, while its electrical conductivity is still belong to the insolating region. Therefore, the 1D-2D hybrid nanofillers show significant potential as novel and effective additives for next generation electronic devices.

Acknowledgements

The authors are grateful for the financial support by the National Natural Science Foundation of China (No. 51303034), Natural Science Foundation of Ningbo (No.Y40307DB05), Natural Science Foundation of Guangxi (No.2014GXNSFBA118034), and Guangxi Universities Scientific Research Project (No. YB2014165).

References

1 M. A. Rafiee, J. Rafiee, Z. Wang, H. Song, Z.-Z. Yu and N. Koratkar, *ACS nano*, 2009, 3, 3884-3890.
2 J. Jia, X. Sun, X. Lin, X. Shen, Y.-W. Mai and J.-K. Kim, *ACS nano*, 2014.
3 S. Liu, H. Yan, Z. Fang and H. Wang, *Compos. Sci. Technol.*, 2014, 90, 40-47.

4 Q. Liang, X. Yao, W. Wang, Y. Liu and C. P. Wong, *ACS nano*, 2011, 5, 2392-2401.
5 I. Zaman, T. T. Phan, H.-C. Kuan, Q. Meng, L. T. Bao La, L. Luong, O. Youssf and J. Ma, *Polymer*, 2011, 52, 1603-1611.
6 N. D. Luong, U. Hippi, J. T. Korhonen, A. J. Soininen, J. Ruokolainen, L.-S. Johansson, J.-D. Nam, L. H. Sinh and J. Seppälä, *Polymer*, 2011, 52, 5237-5242.
7 Z. Xu and C. Gao, *Macromolecules*, 2010, 43, 6716-6723.
8 M. J. McAllister, J.-L. Li, D. H. Adamson, H. C. Schniepp, A. A. Abdala, J. Liu, M. Herrera-Alonso, D. L. Milius, R. Car and R. K. Prud'homme, *Chem. Mater.*, 2007, 19, 4396-4404.
9 X. Pu, H.-B. Zhang, X. Li, C. Gui and Z.-Z. Yu, *RSC Adv.*, 2014, 4, 15297-15303.
10 Y. Wang, J. Yu, W. Dai, Y. Song, D. Wang, L. Zeng and N. Jiang, *Polym. Compos.*, 2014, DOI: 10.1002/pc.22972.
11 A. Muthukaruppan, S. Krishnamoorthy and P. Prabunathan, *RSC Adv.*, 2014.
12. L. Yang, S. L. Phua, J. K. Teo, C. L. Toh, S. K. Lau, J. Ma and X. Lu, ACS *Appl. Mater. Inter.*, 2011, 3, 3026-3032.
13. L. Yang, S. L. Phua, C. L. Toh, L. Zhang, H. Ling, M. Chang, D. Zhou, Y. Dong and X. Lu, *RSC Adv.*, 2013, 3, 6377.
14. H. J. Salavagione, G. Martínez and G. Ellis, *Macromol. Rapid Commun.*, 2011, 32, 1771-1789.
15. N. Yousefi, X. Lin, Q. Zheng, X. Shen, J. R. Pothnis, J. Jia, E. Zussman and J.-K. Kim, *Carbon*, 2013, 59, 406-417.
16. Y.T. Liu, M. Dang, X. M. Xie, Z. F. Wang and X. Y. Ye, *J. Mater. Chem.*, 2011, 21, 18723-18729.
17. W. D. Zhang, I. Y. Phang and T. Liu, *Adv. Mater.*, 2006, 18, 73-77.
18. H. N. Tien, T. V. Cuong, B.-S. Kong, J. S. Chung, E. J. Kim and S. H. Hur, *J. Mater. Chem.*, 2012, 22, 8649-8653.
19. A. Yu, P. Ramesh, X. Sun, E. Bekyarova, M. E. Itkis and R. C. Haddon, *Adv. Mater*., 2008, 20, 4740-4744.
20. H. Palza, B. Reznik, M. Wilhelm, O. Arias and A. Vargas, *Macromol. Mater. Eng.,* 2012, 297, 474-480.
21. D. Liu, S. Xie, X. Yan, L. Ci, F. Shen, J. Wang, Z. Zhou, H. Yuan, Y. Gao and L. Song, *Chem. Phys. Lett.,* 2003, 375, 269-272.
22. C. Liang, G. Meng, L. Zhang, Y. Wu and Z. Cui, *Chem. Phys. Lett.,* 2000, 329, 323-328.
23. G. Meng, L. Zhang, Y. Qin, C. Mo and F. Phillipp, *Nanostruct. Mater.,* 1999, 12, 1003-1006.
24. H. Zhang, E. López-Honorato, A. Javed, X. Zhao, J. Tan and P. Xiao, *J. Eur. Ceram. Soc.,* 2012, 32, 1775-1786.
25. A. Meng, Z. Li, J. Zhang, L. Gao and H. Li, *J. Cryst. Growth,* 2007, 308, 263-268.
26. S. Y. Yang, C. C. M. Ma, C. C. Teng, Y. W. Huang, S. H. Liao, Y. L. Huang, H. W. Tien, T. M. Lee and K. C. Chiou, *Carbon*, 2010, 48, 592-603.
27. C. Lin and D. Chung, *Carbon*, 2009, 47, 295-305.
28. M. Biercuk, M. C. Llaguno, M. Radosavljevic, J. Hyun, A. T. Johnson and J. E. Fischer, *Appl. Phys. Lett.,* 2002, 80, 2767-2769.
29. S. Y. Yang, W. N. Lin, Y. L. Huang, H. W. Tien, J. Y. Wang, C. C. M. Ma, S. M. Li and Y. S. Wang, *Carbon,* 2011, 49, 793-803.
30. S. Shenogin, L. Xue, R. Ozisik, P. Keblinski and D. G. Cahill, *J. Appl. Phys.,* 2004, 95, 8136-8144.
31. S. Ganguli, A. K. Roy and D. P. Anderson, *Carbon*, 2008, 46, 806-817.
32. N. Grassie, M. I. Guy and N. H. Tennent, *Polym. Degrad. Stab.,* 1986, 14, 125-137.
33. C. Zhang, W. W. Tjiu, T. Liu, W. Y. Lui, I. Y. Phang and W.-D. Zhang, *J. Phys. Chem. B,* 2011, 115, 3392-3399.
34. S. Lu, S. Li, J. Yu, Z. Yuan and B. Qi, *RSC Adv.*, 2013, 3, 8915-8923.
35. W. S. Saw and M. Mariatti, *J. Mater. Sci.,* 2012, 23, 817-824.
36. Y. Zhao and E. V. Barrera, *Adv. Funct. Mater.,* 2010, 20, 3039-3044.
37. Y. Bai and L. Jin, Journal of Physics D: *Appl, Phys.,* 2008, 41, 152008.
38. P. R. Thakre, Y. Bisrat and D. C. Lagoudas, *J. Appl. Polym. Sci.,* 2010, 116, 191-202.
39. F. Gardea and D. C. Lagoudas, *Compos. Part B*, 2014, 56, 611-620.
40. S. Barrau, P. Demont, A. Peigney, C. Laurent and C. Lacabanne, *Macromolecules*, 2003, 36, 5187-5194.
41. C. Min, D. Yu, J. Cao, G. Wang and L. Feng, *Carbon*, 2013, 55, 116-125.
42. A. Soulintzis, G. Kontos, P. Karahaliou, G. Psarras, S. Georga and C. Krontiras, *J. Polym. Sci. Part B: Polym. Phys.*, 2009, 47, 445-454.
43. Y. Deng, Y. Zhang, Y. Xiang, G. Wang and H. Xu, *J. Mater. Chem.*, 2009, 19, 2058-2061.

